

Critical-Current Measurements on ITER Nb₃Sn Strands: Effect of Temperature

L. F. Goodrich, N. Cheggour, J. W. Ekin, and T. C. Stauffer

Abstract—Transport critical-current (I_c) measurements were made on commercial multifilamentary Nb₃Sn strands at temperatures (T) from 4 to 17 K and magnetic fields (H) from 0 to 14 T. Samples investigated were taken from the stage 1 pre-production strand for the central solenoid of the International Thermonuclear Experimental Reactor (ITER) project. Specimens were mounted on a three-turn Ti-6Al-4V (percent by mass) mandrel, which was a shorter version of the standard ITER critical-current mandrel. The measurements covered the range of critical currents from less than 0.1 A to over 700 A. To verify the accuracy of the variable-temperature measurements, we compared critical-current values obtained on a specimen that was immersed in liquid helium at 5 K to those measured on the same specimen in flowing helium gas at the same temperature. This comparison indicated that specimen temperature was controlled to within 60 mK during the measurements. The critical-current data presented include electric-field versus temperature (E - T) characteristics, $I_c(T)$ at constant H , and extrapolated effective upper critical field as a function of temperature. These data are part of what is needed for the ITER strand characterization.

Index Terms—Critical-current density, ITER, niobium-tin, superconducting wires, variable temperature.

I. INTRODUCTION

VARIABLE temperature measurements are needed to determine the temperature margin of superconducting strands. The temperature margin is defined as the difference between the operating temperature and the temperature at which the operating current equals the critical current (I_c). When a magnet is operating, transient excursions in magnetic field (H) or current (I) are not expected; however, many events or effects can cause transient excursions to higher temperatures (T), such as wire motion, ac losses, and radiation. Hence, temperature margin is a key strand characteristic.

We made transport critical-current measurements on Nb₃Sn strands at temperatures from 4 to 17 K and magnetic fields from 0 to 14 T. The strands investigated were two developmental wires made by two U.S. manufacturers for the International Thermonuclear Experimental Reactor (ITER) central solenoid magnet. The wire diameter was 0.83 mm and the Cu/non-Cu ratio was about 1.1. Further information on the designs of these

two strands was not disclosed for competitive reasons. The measurements covered the range of critical currents from less than 0.1 A to over 700 A, with an electric field (E) criterion of 10 $\mu\text{V}/\text{m}$. Data acquired include electric-field/current (E - I) characteristics at constant H and T , electric-field/temperature (E - T) characteristics at constant I and H , $I_c(H)$ at constant T , and $I_c(T)$ at constant H . These data are needed to determine the temperature margin of magnets (especially for applications that use cable-in-conduit conductor) and performance data for cryogen-free applications. The measured I_c at 10 $\mu\text{V}/\text{m}$, 4.2 K, and 12 T was 278 A (n -value 33) for specimen A taken from one of the two strands, and was 203 A (n -value 23) for specimen B taken from the other strand. A more optimal heat treatment was later found for the second strand that increased its I_c at 12 T to closer to that of the first strand. Three other specimens of each strand were measured at 4.2 K, and the critical currents of these additional specimens were close to those of the respective variable temperature specimens.

II. PROCEDURE

A fairly detailed description of our variable-temperature apparatus is given in reference [1]. One difference from that description is that the present measurements were made on a coil-geometry specimen [2], in a solenoidal magnet; however, the basic concept is the same. One further change since that publication is that we now control the temperature of each current contact with separate temperature controllers rather than controlling one contact and using a balance heater to keep the other at the same temperature. Magnetoresistance corrections were made to all thermometers (metal oxy-nitride resistors) [3], [4]. These are the first measurements made using a new version of our variable temperature cryostat designed to fit into smaller-bore, higher-field magnets (52 mm bore, 14 T at 4.2 K and 16 T at 2.2 K).

The specimen was reacted and measured on a thin-walled Ti-6Al-4V (percent by mass, Ti-6-4) tube. The Cr plating was removed from the specimens prior to the heat treatment. The Ti-6-4 tube was the same as that used by the ITER project [5], except that the ends had been machined so that there were only three turns between the current contacts (about 30 cm active length) and the current contacts were longer. These slight modifications, which only concerned the sample length, were made for better temperature homogeneity along the length of the sample. The voltage taps were separated by 10 cm. No copper plating, solder (except for the voltage taps), or epoxy was applied to the specimen between the current contacts. The apparent I_c (shunting current) at 10 $\mu\text{V}/\text{m}$, measured when the sample was normal, was less than 0.1 A at 18 K and 0 T and

Manuscript received August 29, 2006. This work was supported in part by the U.S. Department of Energy, Office of Fusion Energy Sciences, under Grant DE-FC02-93ER54186.

The authors are with the National Institute of Standards and Technology, Boulder, CO 80305 USA (e-mail: goodrich@boulder.nist.gov).

Color versions of one or more of the figures in this paper are available online at <http://ieeexplore.ieee.org>.

Digital Object Identifier 10.1109/TASC.2007.897225

TABLE I
COMPARISON OF I_c MEASUREMENTS IN GAS AND LIQUID AT 5 K

SPECIMEN A			SPECIMEN B	
$\mu_0 H$ (T)	I_c (A, liquid)	I_c (A, gas) - I_c (A, liquid)	I_c (A, liquid)	I_c (A, gas) - I_c (A, liquid)
4	-	-	745	-1.9
5	-	-	611	-0.6
6	660	-3.8	507	1.0
7	560	-3.0	425	1.6
8	476	-1.1	358	1.7
9	405	0.1	302	1.7
10	345	0.6	255	1.5
11	292	1.0	215	1.4
12	246	1.1	179	1.3
13	206	1.2	149	1.2
14	171	1.3	122	1.0

less than 0.01 A at 12 K and 13 T, indicating that the shunted current in the mandrel and specimen matrix was very low.

Complete E - I characteristics were measured step-wise at many temperatures and certain currents. From these data, E - T characteristics could also be generated at constant currents. Two or three determinations were made at most of the current set-points. The current set-points were approximately every 1, 1.5, 2, 3, or 4 A, depending on the level of current. Our current supply could repeat the set-points to within about 0.03 A.

A conservative estimate of the standard uncertainty in these Nb₃Sn critical current measurements at 4.2 K due to systematic effects is 2.5%, and that due to random effects is 0.6%. The uncertainty at temperatures above 4.2 K is higher because of the increased sensitivity of critical current to temperature, magnetic field, and strain state.

III. CRITICAL CURRENT VERSUS TEMPERATURE

To verify the accuracy of measurements taken at variable temperatures, we compared critical-current values (up to over 650 A) of a specimen measured while immersed in liquid helium (“liquid”) to those on the same specimen measured in a helium gas flow (“gas”). For the rest of this paper, data from the first case will be referred to as *liquid* data and data from the second referred to as *gas* data. Table I compares I_c values measured in *gas* and *liquid* at 5 K for various magnetic fields and both specimens. Differences in I_c were less than 1%. By comparing I_c values we obtain the apparent difference in specimen temperature, which is a direct indication of our ability to control specimen temperature during measurements in *gas*. If the differences given in Table I were expressed in terms of temperature, using the $I_c(H, T)$ dependence, they would be less than 60 mK.

Measurements of I_c versus T at magnetic fields from 0 to 14 T are shown in Fig. 1 for specimen A and in Fig. 2 for specimen B. Data cover the whole range of critical currents from less than 0.01 A to over 700 A with an electric-field criterion of 10 $\mu\text{V}/\text{m}$; however, the points below 6 A were not shown to reduce the overlap of curves. For specimen B, measurements were made at 4.2 K and at integer temperatures above 4.2 K. For specimen A, odd temperatures above 8 K were skipped. Data

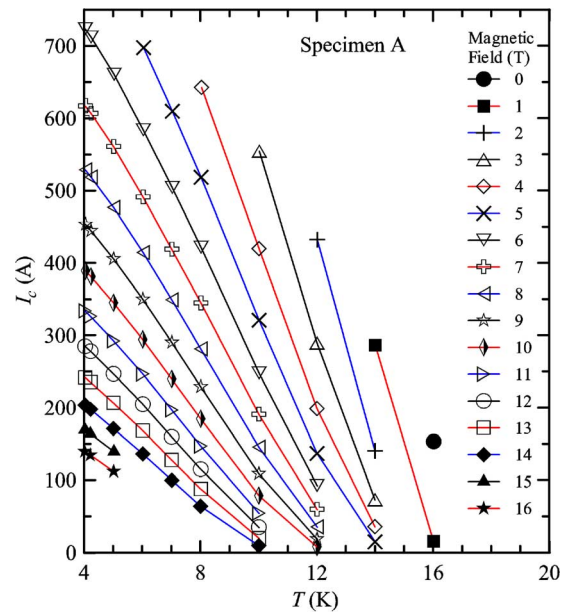


Fig. 1. Linear plot of critical current versus temperature at various magnetic fields for specimen A. The lines connecting data points are to guide the eye.

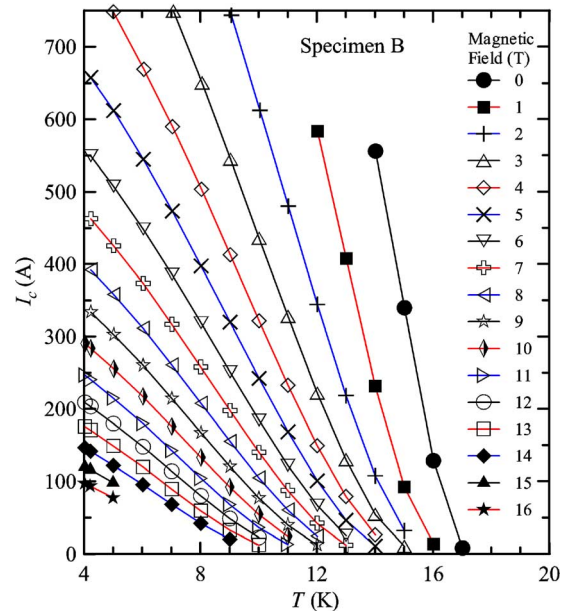


Fig. 2. Linear plot of critical current versus temperature at various magnetic fields for specimen B. The lines connecting data points are to guide the eye.

at 5 K and below are *liquid* data, and those above 5 K are *gas* data. Variable-temperature measurements in *gas* at 15 and 16 T were not made since the magnet had to be operated near 2.2 K to reach these fields. For I_c above 100 A, the I_c versus T curves are nearly linear. At low magnetic fields, *gas* data were limited to currents below 650 or 750 A, depending on how stable the specimen was. Specimen B was slightly more stable than specimen A, especially below 4 T. The stability of the specimen depends on many parameters, including the random chance of a lower I_c for either end of the specimen, outside the middle 10 cm. The curves below about 30 A exhibit a tail at high temperatures.

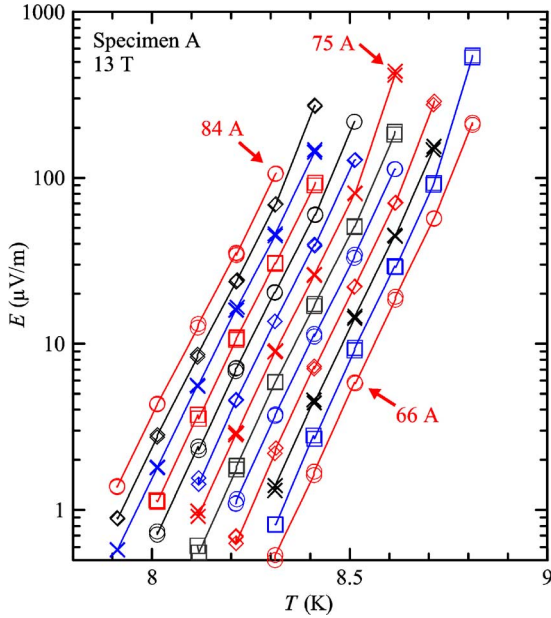


Fig. 3. Semi-logarithmic plot of electric field versus temperature at 13 T and constant currents from 66 to 84 A with current steps of 1.5 A for specimen A. The lines connecting data points are to guide the eye.

IV. E - I AND E - T CURVES

E - I characteristics were measured at temperatures from 6.8 to 9.2 K in steps of 0.1 K for specimen A and from 6 to 8.5 K for specimen B, in a magnetic field of 13 T. We did not hold the current constant and ramp the temperature to obtain the E - T curves more directly because that would not be as efficient and the duty cycle of the current would be too high. This covered a range of currents around 75 A, which is the approximate strand design current. A specific set of sample currents was used. The current steps were every 1.5 A for currents from 60 to 108 A. Two or three E - I curves were acquired up to the highest E possible below the quench (abrupt and irreversible transition to the normal state) at each temperature. These data were combined and sorted by temperature to obtain E - T characteristics for each specimen.

Fig. 3 (specimen A) and Fig. 4 (specimen B) show semi-logarithmic E - T characteristics at currents from 66 to 84 A in a magnetic field of 13 T. The symbols are repeated in a regular pattern in order to use a limited number of symbols that are easily distinguished. Plots of E - T characteristics at constant currents and fixed magnetic field directly indicate the temperature margin of a conductor.

The n -value is the slope of the full-logarithmic plot of the E - I curve [2], and is a figure of merit for a conductor [6]. The semi-logarithmic curves of E - T in Figs. 3 and 4 have a shape similar to that of the E - I curves, which suggests that the E - T curves could also be approximated on a full-logarithmic scale by a constant slope defined as the m -value [7], [8]. We chose to plot the E - T curves on a semi-logarithmic scale in order to place more meaningful tick marks along the T -axis. Also, over the very narrow range of the T -axis, there is not much visible difference between linear and logarithmic scales. The E - T curves plotted on a full-logarithmic scale are slightly straighter.

For specimen A, the n -value of the E - I curve near 75 A and 8.3 K is about 21, and the m -value of the E - T curve near that

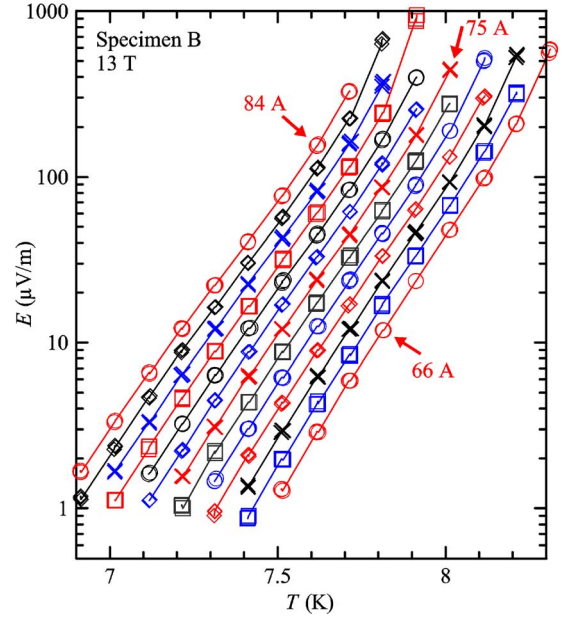


Fig. 4. Semi-logarithmic plot of electric field versus temperature at 13 T and constant currents from 66 to 84 A with current steps of 1.5 A for specimen B. The lines connecting data points are to guide the eye.

same point is about 92. For specimen B, the n -value of the E - I curve near 75 A and 7.5 K is about 17, and the m -value of the E - T curve near that same point is about 50. There is no simple relationship between the n -value and the m -value, but the higher n -value for specimen A, in comparison to specimen B, is also reflected in a higher m -value, as can be seen by comparing Figs. 3 and 4.

The highest E below quench appears to be quantized because the current set-points were quantized, to allow for E - T curves at constant I . This, combined with the differences in m -values, makes it hard to compare highest E below quench for these two specimens. However, these data suggest that specimen B is slightly more stable than specimen A. The significantly higher m -values for specimen A, compared to those of specimen B, may be an important factor that lowered the apparent stability of specimen A.

V. EFFECTIVE UPPER CRITICAL FIELD

The effective upper critical field (B_{c2}^*), the field at which the pinning force density (F_p) extrapolates to zero, can be estimated with $I_c(H, T)$. These data were acquired with the sample at only one strain state; that of the sample cooled from room temperature on the Ti-6Al-4V holder. The differential thermal contraction between the sample and the mandrel is expected to tighten and stretch the sample as it is cooled. This will remove some of the pre-compression on the Nb₃Sn arising from the differential thermal contraction among the composite constituents. Following the pinning-force fitting procedure described in [9], p , q , η , and ν were determined using the following equations. The pinning force density scaling law is given by

$$F_p = J_c \times B = K \left(\frac{B}{B_{c2}^*} \right)^p \left(1 - \left(\frac{B}{B_{c2}^*} \right) \right)^q \quad (1)$$

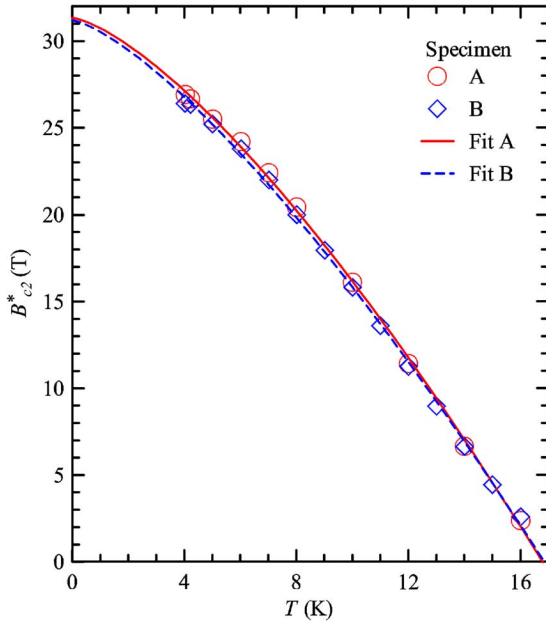


Fig. 5. Effective upper critical field (B_{c2}^*) versus temperature for the two Nb₃Sn samples.

where J_c is the critical-current density, B is the magnetic flux density, K is a function of B_{c2}^* , and p and q are constants. The dependence of K is given by [10]

$$K \propto (B_{c2}^*)^\eta \quad (2)$$

where η is a temperature scaling constant (not related to the n -value). B_{c2}^* can be parameterized by the following equation:

$$B_{c2}^*(T) = B_{c2}^*(0) \left(1 - \left(\frac{T}{T_c^*} \right)^\nu \right) \quad (3)$$

where ν is a constant, $B_{c2}^*(0)$ is the B_{c2}^* at zero temperature, and T_c^* is the effective critical temperature at which B_{c2}^* extrapolates to zero. $B_{c2}^*(T)$ is given in Fig. 5 for the two specimens. The parameter values for specimen A are $p = 0.56$, $q = 1.86$, $\eta = 2.15$, $\nu = 1.40$, $T_c^* = 16.79$ K, $B_{c2}^*(0) = 31.3$ T, and $B_{c2}^*(4.2$ K) = 26.9 T. The parameter values for specimen B are $p = 0.51$, $q = 1.88$, $\eta = 2.15$, $\nu = 1.36$, $T_c^* = 16.85$ K, $B_{c2}^*(0) = 31.2$ T, and $B_{c2}^*(4.2$ K) = 26.5 T. The small differences in B_{c2}^* and T_c^* for the two specimens are well within the uncertainty of the extrapolation. It is noteworthy that all of the fitting parameters are very similar for the two strands, even though the strands were made by different manufacturers.

VI. CONCLUSION

We fit the pinning force density to estimate the parameterization of $I_c(H, T)$ for two ITER developmental Nb₃Sn strands

using data over a wide range of current, temperature, and magnetic field. The fitting parameters were very similar for the two strands, and were within the expected range of values for Nb₃Sn wires. Complementary to this work, measurements of the strain effect on other B specimens are reported in [11]. The common fitting parameters for the field dependence of the pinning force were very similar for both variable temperature and variable strain measurements [9]. Any possible limitations to extrapolating the scaling law were not examined in this work.

ACKNOWLEDGMENT

The authors thank Dr. Joseph Minervini and his staff at the Massachusetts Institute of Technology, Plasma Science and Fusion Center for their contributions and support of our project.

Contribution of NIST, not subject to copyright in the United States. Certain commercial equipment or materials mentioned in this paper may be indirectly identified by their particular properties. Such identification does not imply recommendation or endorsement by NIST, nor does it imply that the equipment or materials identified are necessarily the best available for the purpose.

REFERENCES

- [1] L. F. Goodrich and T. C. Stauffer, "Hysteresis in transport critical-current measurements of oxide superconductors," *NIST J. Res.*, vol. 106, pp. 657–690, 2001.
- [2] L. F. Goodrich and F. R. Fickett, "Critical current measurements: A compendium of experimental results," *Cryogenics*, vol. 22, pp. 225–241, 1982.
- [3] L. F. Goodrich and T. C. Stauffer, "Variable temperature critical-current measurements on a Nb-Ti wire," *Adv. Cryo. Eng. Materials*, vol. 50B, pp. 338–345, 2004.
- [4] B. L. Brandt, D. W. Liu, and L. G. Rubin, "Low temperature thermometry in high magnetic fields. VII. Cernox sensors to 32 T," *Rev. Sci. Instrum.*, vol. 70, pp. 104–110, 1999.
- [5] P. Bruzzone, H. H. J. ten Kate, M. Nishi, A. Shikov, J. Minervini, and M. Takayasu, "Bench mark testing of Nb₃Sn strands for the ITER model coil," *Adv. Cryo. Eng. Materials*, vol. 42B, pp. 1351–1358, 1997.
- [6] W. H. Warnes and D. C. Larbalestier, "Determination of the average critical current from measurements of the extended resistive transition," *IEEE Trans. Magn.*, vol. 23, pp. 1183–1187, 1987.
- [7] E. Y. Klimenko, N. N. Martovetsky, and S. I. Novikov, "Stability of the real superconductors," in *Proc. 9th International Conf. on Magnet Technology*, C. Marinucci and P. Weymuth, Eds., Swiss Institute for Nuclear Research, Switzerland, 1986, pp. 581–583.
- [8] N. N. Martovetsky, "Some aspects of modern theory of applied superconductivity," *IEEE Trans. Magn.*, vol. 25, pp. 1692–1697, 1989.
- [9] N. Cheggour and D. P. Hampshire, "The unified strain and temperature scaling law for the pinning force density of bronze-route Nb₃Sn wires in high magnetic fields," *Cryogenics*, vol. 42, pp. 299–309, 2002.
- [10] W. A. Fietz and W. W. Webb, "Hysteresis in superconducting alloys-temperature and magnetic field dependence of dislocation pinning in niobium alloys," *Phys. Rev.*, vol. 178, pp. 657–667, 1969.
- [11] N. Cheggour, J. W. Ekin, and L. F. Goodrich, "Critical-current measurements on ITER Nb₃Sn strands: Effect of axial tensile strain," *IEEE Trans. Appl. Supercond.*, submitted for publication.